Int. J. Advanced Design and Manufacturing Technology, 2025, Vol. 18, No. 2, pp. 71-80

DOI: 10.71644/admt.2025.1106718 *ISSN: 2252-0406* *https://admt.isfahan.iau.ir*

On the Analysis of Two-Dimensional Functionally Graded Rotating Thick Hollow Cylinder

Mostafa Omidi Bidgoli[1, *]
Department of Mechanical Engineering, Islamic Azad University, Badroud branch, Badroud, Iran
E-mail: mostafaomidibidgoli@gmail.com
*Corresponding author

Mohammad Hosseini[2], Ali Fata[3]
Department of Mechanical Engineering, University of Hormozgan, Bandar Abbas, Iran
E-mail: mohammad.hosseini@hormozgan.ac.ir, fata.ali@gmail.com

Received: 10 September 2024, Revised: 25 February 2025, Accepted: 18 March 2025

Abstract: Rotary components are widely used in industries. There is both mechanical and thermal loading in most rotating cylinder applications. On the other hand, functionally graded material has better performance under different loads. Therefore, a finite length two dimensional functionally graded material (2D-FGM) thick hollow cylinder under angular velocity is investigated, in this research. Volume fraction distribution of functionally graded material and geometry of the cylinder are axisymmetric but not uniform along the radial and axial directions. The finite element method based on Rayliegh-Ritz energy formulation is applied to obtain the governing Equation and associated boundary conditions of a 2D-FG thick hollow cylinder. Using this method, the effects of the power law exponents and angular velocity on the displacements and distribution of stresses are investigated for simply supported 2D-FG thick hollow cylinder. The results indicate that 2D-FGM facilitates improved design, allowing for better control of both maximum stresses and stress distribution through material distribution.

Keywords: 2D Functionally Graded Material, FEM, Rotating Cylinder, Thick Hollow Cylinder

Biographical notes: Mostafa Omidi Bidgoli is an assistant professor and accomplished mechanical engineer specializing in solid mechanics, with expertise in FGM, stress and strain analysis, and creep analysis. He received his Ph.D. in Mechanical Engineering from the University of Kashan in 2019. He is an assistant professor at IAU, Badroud branch. **Mohammad Hosseini** is an assistant professor and accomplished mechanical engineer specializing in solid mechanics, with expertise in nano-structures, MEMS, and NEMS, stress analysis, and finite element methods. He received his Ph.D. in Mechanical Engineering from Shahid Chamran University of Ahvaz in 2017. **Ali Fata** is an associate professor of Mechanical Engineering at Hormozgan University, specializing in Manufacturing Engineering and advanced materials processing. He received his Ph.D. in Mechanical Engineering from Amir Kabir University in 2012.

Research paper

1 INTRODUCTION

Rotating cylinders with functionally graded materials (FGMs) have attracted much attention recently as an innovation in materials, engineering, and structural design. FGMs are heterogeneous composite materials whose mechanical properties vary continuously between several different materials. Also, the rotary cylinder is widely used in various industries. Functionally graded cylinders are used in internal combustion engines, gas turbines, medicine, etc. The presence of variable stresses and thermal fields in rotating cylinders requires careful design and the use of materials with specific properties. FGMs have the ability to adapt to these challenges by gradually changing the composition and properties of the materials along the design. In most rotating cylinder applications, there is both mechanical and thermal loading. The cylinder can be made of functionally graduated to perform optimally under different loads. It is necessary to theoretically examine the behavior of the functionally graded structure before the construction process, considering the high costs of laboratory tests. In the last few years, much research has been carried out to investigate the behavior of the rotating functional graduated cylinder, which will be discussed in the following.

Shi and Xie [1] presented an exact solution for a hollow FG cylinder under the simultaneous action of an applied magnetic field and internal pressure. They analyzed residual stresses caused by unloading internal pressure and the effect of some parameters on the plastic zone size. Li et al. [2] derived the governing Equation of a functionally graded cylinder or circular disk. The structure was under axisymmetric mechanical and thermal loads. They investigate the effect of some parameters, such as the inhomogeneity parameter, thermal and magnetic fields, internal pressure, and rotating velocity. Using the Pseudospectral Chebyshev Method, Yarimpabuç and Çalişkan [3] investigated the elastic behavior of FG rotating hollow cylindrical pressure vessels. Daghigh et al. [4] discussed the time-dependent behavior of FGM rotating disks of variable thickness subject to mechanical load and uniform temperature. In the frameworks of first-order shear deformation theory, Sedighi et al. [5] studied the time-dependent creep behavior of thick-walled cylinders under internal pressure, and heat flux at the inner and outer surfaces has been investigated. Omidi Bidgole et al. [6] used first-order shear deformation theory to analyze transient stress and deformations of short-length FG rotating cylinders subjected to thermal and mechanical loads on a friction bed. Based on the finite element method, Maitra et al. [7] presented an analysis for rotating truncated radially FG conical shells under constant and variable internal pressure. Creep analysis of an FG rotating disc of variable thickness was discussed by Saadatfar et al. [8]. They explained the effect of design parameters on the creep behavior of the disc. Using the Biot poroelastic law, Babaei et al. [9] derived the governing Equation and discussed the dynamic behavior of the FG-saturated porous rotating thick truncated cone. Xu et al. [10] presented a model to explain elastic wave propagation in a 2D-FG thick hollow cylinder. Yarımpabuç [11] used a closed-form solution to study the transient thermal stress analysis of a radially FG hollow cylinder subjected to high-temperature difference and periodic rotation effect. Jabbari and Zamani Nejad [12] investigated the effect of thermal and mechanical loads on the strain and stress distribution of rotating radially FG shells of variable thickness. Mehditabar et al. [13] studied the mechanical behavior of radially FG rotating hollow cylindrical shells under dynamic loading. Gharibi et al. [14] derived and solved the governing Equation of radially FG rotating thick cylindrical pressure vessels. Jabbari et al. [15] analyzed axially FG rotating thick cylindrical of variable thickness subject to thermo-elastic loads. They used higher-order shear deformation theory and the multilayer method to derive the governing Equation.

Jafari Fesharaki et al. [16] presented a 2D solution for the electro-mechanical behavior of functionally graded piezoelectric hollow cylinders under 2D electro-mechanical loads.

Zafarmand and Hasani [17] studied the elastic behavior of a 2D-FGM rotating disk of variable thickness. They investigate the effect of the thickness profile and material inhomogeneity index on the displacement distribution and stresses. Dai et al. [18] analyzed displacements and stresses of radially FG piezoelectric rotating hollow cylinders. Also, much research has been done on rotating structures in addition to the ones reviewed in this article [19-44].

As can be seen, much research has been done on rotating functionally graduated cylinders. Most of the articles have assumed material changes either in the radial direction or in the axial direction. In this paper, the stress analysis of 2D-FGM rotating thick hollow cylinders has been investigated for the first time. The problem is modeled using 2D axisymmetric elasticity theory and the finite element method based on the Rayleigh-Ritz energy formulation. The influence of power law exponents and rotational velocity on the distribution of displacements and stresses is considered.

2 MATERIAL AND GEOMETRY OF STRUCTURE

Figure 1 shows a thick hollow cylinder, where r and z are the radial, and length axis of cylindrical coordinate system.

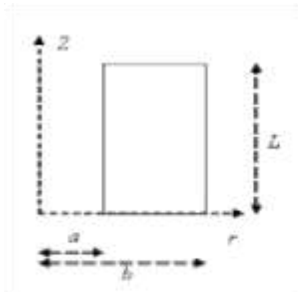

Fig. 1 Geometry of the cylinder.

The inner surface of the cylinder is made of ceramics, and the outer surface is made of metal alloys. Material properties vary through both the radial and axial directions. The volume fraction of constituent materials can be expressed as:

$$\mathrm{Vc}_1 = \left(1-\left(\frac{r-a}{b-a}\right)^{n_r}\right)\left(1-\left(\frac{z}{L}\right)^{n_z}\right) \tag{1}$$

$$\mathrm{Vc}_2 = \left(1-\left(\frac{r-a}{b-a}\right)^{n_r}\right)\left(\frac{z}{L}\right)^{n_z} \tag{2}$$

$$\mathrm{Vm}_1 = \left(\frac{r-a}{b-a}\right)^{n_r}\left(1-\left(\frac{z}{L}\right)^{n_z}\right) \tag{3}$$

$$\mathrm{Vm}_2 = \left(\frac{r-a}{b-a}\right)^{n_r}\left(\frac{z}{L}\right)^{n_z} \tag{4}$$

Therefore, the material properties at each point can be obtained by the linear rule of mixtures as:

$$\mathrm{E} = \mathrm{Ec}_1\mathrm{Vc}_1 + \mathrm{Ec}_2\mathrm{Vc}_2 + \mathrm{Em}_1\mathrm{Vm}_1 + \mathrm{Em}_2\mathrm{Vm}_2 \tag{5}$$

For instance, the volume fraction distribution of the second ceramic and the variation of modulus of elasticity through the cylinder for typical values of $n_r = n_z = 2$ are shown in “Figs. 2 and 3”, respectively. In this case, a=1 m, b=1.5 m, and L=1 m. The essential constituents of the 2D-FGM cylinder are presented in “Table 1”.

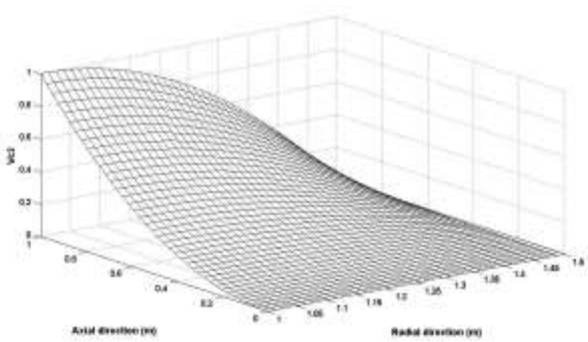

Fig. 2 Volume fraction distribution of second ceramic through the cylinder for $n_r = n_z = 2$.

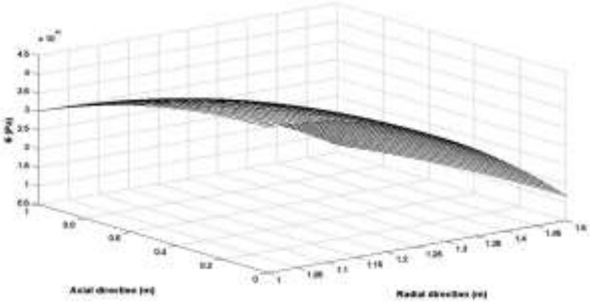

Fig. 3 Distribution of modulus of elasticity through the cylinder for $n_r = n_z = 2$.

Table1 Basic constituent of 2D-FGM cylinder

Constituent	Material	E (GPa)	Density (kg/m3)
m_1	Ti6Al4V	115	4515
m_2	Al 1,100	69	2715
c_1	SiC	440	3210
c_2	Al2O3	300	3470

3 Governing Equations of Rotating Thick Hollow Cylinder

Figure 1 shows a rotating thick hollow cylinder. Based on the axial symmetry assumption, the formulation is reduced to two dimensions. Due to axisymmetric geometry, axisymmetric material properties, and axisymmetric load distribution, the circumferential displacement, shear stresses, and strains in r_θ and θ_z planes are zero. Governing Equations in axisymmetric cylindrical coordinates were obtained as:

$$\frac{\partial \sigma_{rr}}{\partial r} + \frac{(\sigma_{rr}-\sigma_{\theta\theta})}{r} + \frac{\partial \tau_{rz}}{\partial z} + \rho(r,z)\, r\, \omega^2 = 0 \tag{6}$$

$$\frac{\partial \tau_{rz}}{\partial r} + \frac{\partial \sigma_{zz}}{\partial z} + \frac{\tau_{rz}}{r} = 0 \tag{7}$$

Linear strain-displacement relations are:

$$[\varepsilon] = \begin{bmatrix} \varepsilon_{rr} \\ \varepsilon_{\theta\theta} \\ \varepsilon_{zz} \\ \varepsilon_{rz} \end{bmatrix} = \begin{bmatrix} \dfrac{\partial u}{\partial r} \\ \dfrac{u}{r} \\ \dfrac{\partial v}{\partial z} \\ \dfrac{1}{2}\left(\dfrac{\partial u}{\partial z} + \dfrac{\partial v}{\partial r}\right) \end{bmatrix} \tag{8}$$

Where u and v are the radial and axial displacements, respectively. "Eq. (8)" could be rewritten as:

$$[\varepsilon]=[d]\{f\} \qquad \{f\}=\begin{Bmatrix} u \\ v \end{Bmatrix} \tag{9}$$

Where:

$$[d]=\begin{bmatrix} \frac{\partial}{\partial r} & 0 \\ \frac{1}{r} & 0 \\ 0 & \frac{\partial}{\partial z} \\ \frac{1}{2}\frac{\partial}{\partial z} & \frac{1}{2}\frac{\partial}{\partial r} \end{bmatrix}$$

Based on the Hooke's law, the stress-strain relationship is:

$$[\sigma]=\begin{bmatrix} \sigma_{rr} \\ \sigma_{\theta\theta} \\ \sigma_{zz} \\ \tau_{rz} \end{bmatrix}=[D][\varepsilon] \tag{10}$$

Where:

$$[D]=\frac{E}{(1+\upsilon)(1-2\upsilon)} \times \begin{bmatrix} 1-\upsilon & \upsilon & \upsilon & 0 \\ \upsilon & 1-\upsilon & \upsilon & 0 \\ \upsilon & \upsilon & 1-\upsilon & 0 \\ 0 & 0 & 0 & 1-2\upsilon \end{bmatrix}=E\,\mathbf{\Lambda} \tag{11}$$

In "Eq. (11)", E is the Young's modulus, which is a function of r and z components. Also, υ denotes Poisson's ratio, and it is constant.

The cylinder has simply supported boundary conditions, so displacement boundary conditions are as follows:

$$\mathrm{u}(\mathrm{r},0)=\mathrm{u}(\mathrm{r},\mathrm{L})=0 \qquad \text{S-S} \tag{12}$$

4 FINITE ELEMENT MODELLING

The finite element method is used to solve the governing Equations for 2D-FGM thick hollow cylinders. The displacement matrix of each element (e) in terms of the nodal displacement matrix $\{\delta\}$ and shape function $\boldsymbol{N}$ is:

$$\{f\}^{(e)}=\boldsymbol{N}^{(e)}\{\delta\}^{(e)} \tag{13}$$

By substituting "Eq. (13)" into "Eq. (9)", the strain matrix of the element (e) is determined as:

$$\{\varepsilon\}^{(e)}=\boldsymbol{B}^{(e)}\{\delta\}^{(e)} \tag{14}$$

Where $\boldsymbol{B}^{(e)}=[d]\boldsymbol{N}^{(e)}$ is the strain-displacement matrix. $\boldsymbol{N}^{(e)}$ matrix is as follows for the quadratic six nodded triangular element:

$$\boldsymbol{N}=\begin{bmatrix} N_1 & 0 & N_2 & 0 & N_3 & 0 & N_4 & 0 & N_5 & 0 & N_6 & 0 \\ 0 & N_1 & 0 & N_2 & 0 & N_3 & 0 & N_4 & 0 & N_5 & 0 & N_6 \end{bmatrix} \tag{15}$$

Where:

$$N_1=\frac{\left(r_{23}(z-z_3)-z_{23}(r-r_3)\right)\left(r_{46}(z-z_6)-z_{46}(r-r_6)\right)}{\left(r_{23}z_{13}-z_{23}r_{13}\right)\left(r_{46}z_{16}-z_{46}r_{16}\right)}$$

$$N_2=\frac{\left(r_{31}(z-z_1)-z_{31}(r-r_1)\right)\left(r_{54}(z-z_4)-z_{54}(r-r_4)\right)}{\left(r_{31}z_{21}-z_{31}r_{21}\right)\left(r_{54}z_{24}-z_{54}r_{24}\right)}$$

$$N_3=\frac{\left(r_{21}(z-z_1)-z_{21}(r-r_1)\right)\left(r_{56}(z-z_6)-z_{56}(r-r_6)\right)}{\left(r_{21}z_{31}-z_{21}r_{31}\right)\left(r_{56}z_{36}-z_{56}r_{36}\right)} \tag{16}$$

$$N_4=\frac{\left(r_{31}(z-z_1)-z_{31}(r-r_1)\right)\left(r_{23}(z-z_3)-z_{23}(r-r_3)\right)}{\left(r_{31}z_{41}-z_{31}r_{41}\right)\left(r_{23}z_{43}-z_{23}r_{43}\right)}$$

$$N_5=\frac{\left(r_{31}(z-z_1)-z_{31}(r-r_1)\right)\left(r_{21}(z-z_1)-z_{21}(r-r_1)\right)}{\left(r_{31}z_{51}-z_{31}r_{51}\right)\left(r_{21}z_{51}-z_{21}r_{51}\right)}$$

$$N_6 = \frac{\left(r_{21}\left(z - z_1\right) - z_{21}\left(r - r_1\right)\right)\left(r_{23}\left(z - z_3\right) - z_{23}\left(r - r_3\right)\right)}{\left(r_{21}z_{61} - z_{21}r_{61}\right)\left(r_{23}z_{63} - z_{23}r_{63}\right)}$$

$$r_{ij} = r_i - r_j, \quad z_{ij} = z_i - z_j$$

Where r_i and z_i are the radial and axial coordinates of the i[th] node, respectively.

And $\boldsymbol{B}^{(e)}$ matrix is:

$$\boldsymbol{B} = \begin{bmatrix} \frac{\partial N_1}{\partial r} & 0 & \frac{\partial N_2}{\partial r} & 0 & \frac{\partial N_3}{\partial r} & 0 & \frac{\partial N_4}{\partial r} & 0 & \frac{\partial N_5}{\partial r} & 0 & \frac{\partial N_6}{\partial r} & 0 \\ \frac{1}{r}N_1 & 0 & \frac{1}{r}N_2 & 0 & \frac{1}{r}N_3 & 0 & \frac{1}{r}N_4 & 0 & \frac{1}{r}N_5 & 0 & \frac{1}{r}N_6 & 0 \\ 0 & \frac{\partial N_1}{\partial z} & 0 & \frac{\partial N_2}{\partial z} & 0 & \frac{\partial N_3}{\partial z} & 0 & \frac{\partial N_4}{\partial z} & 0 & \frac{\partial N_5}{\partial z} & 0 & \frac{\partial N_6}{\partial z} \\ \frac{1}{2}\frac{\partial N_1}{\partial z} & \frac{1}{2}\frac{\partial N_1}{\partial r} & \frac{1}{2}\frac{\partial N_2}{\partial z} & \frac{1}{2}\frac{\partial N_2}{\partial r} & \frac{1}{2}\frac{\partial N_3}{\partial z} & \frac{1}{2}\frac{\partial N_3}{\partial r} & \frac{1}{2}\frac{\partial N_4}{\partial z} & \frac{1}{2}\frac{\partial N_4}{\partial r} & \frac{1}{2}\frac{\partial N_5}{\partial z} & \frac{1}{2}\frac{\partial N_5}{\partial r} & \frac{1}{2}\frac{\partial N_6}{\partial z} & \frac{1}{2}\frac{\partial N_6}{\partial r} \end{bmatrix} \tag{17}$$

Which the components of $\boldsymbol{B}^{(e)}$ matrix are presented in Appendix A.
The material inhomogeneity of the FG hollow cylinder can be defined using nodal values. Consequently, a graded finite element approach can be utilized to accurately capture smooth variations in material properties at the element level. FGM modeling using graded elements yields more precise results than partitioning the solution domain into homogeneous elements. So, shape functions similar to those of the displacement components can be used:

$$E = \sum_{i=1}^{6} E_i \ N_i = \square \ \boldsymbol{\Xi} \tag{18}$$

$$\rho = \sum_{i=1}^{6} \rho_i \ N_i = \square \ \mathfrak{R} \tag{19}$$

where E_i and ρ_i are the modulus of elasticity and mass density corresponding to i[th] node. □ , $\boldsymbol{\Xi}$ and $\mathfrak{R}$ are vectors of shape functions, modulus of elasticity, and mass densities of each element, respectively, and are defined as follows:

$$\mathrm{N} = [N_1 \quad \dots \quad N_6]_{1\times 6}, \\ \boldsymbol{\Xi} = [E_1 \quad \dots \quad E_6]^T{}_{1\times 6}, \\ \rho = [\rho_1 \quad \cdots \quad \rho_6]^T{}_{1\times 6} \tag{20}$$

Therefore, "Eq. (11)" may be rewritten as:

$$\mathbf{D} = \square \ \boldsymbol{\Xi} \boldsymbol{\Lambda} \tag{21}$$

Based on the principle of minimum potential energy and the Rayleigh-Ritz method, governing Equations can be derived. The total potential energy of the rotating 2D-FGM thick hollow cylinder can be written as:

$$\Pi^{(e)} = \frac{1}{2}\int_{V^{(e)}} \left(\boldsymbol{\varepsilon}^{(e)}\right)^T \boldsymbol{\sigma}^{(e)} dV - \int_{A^{(e)}} (\boldsymbol{q})^T \Gamma dV = \\ \frac{1}{2}\int_{V^{(e)}} \left(\boldsymbol{\delta}^{(e)}\right)^T \boldsymbol{B}^T (\boldsymbol{\Xi\Lambda}) \boldsymbol{B}\, \boldsymbol{\delta}^{(e)} dV - \\ \int_{A^{(e)}} \left(\boldsymbol{\delta}^{(e)}\right)^T \boldsymbol{N}^T \Gamma dV \tag{22}$$

Utilizing the principle of minimum total potential energy leads to:

$$\frac{\partial \Pi^{(e)}}{\partial\left(\boldsymbol{\delta}^{(e)}\right)^T} = 0 \\ \Rightarrow \left(\int_{V^{(e)}} \mathbf{B}^T (\square\ \boldsymbol{\Xi\Lambda}) \mathbf{B} dV\right) \boldsymbol{\delta}^{(e)} = \int_{A^{(e)}} \mathbf{N}^T \Gamma dV \tag{23}$$

In compact form:

$$\mathbf{K}^{(e)} \boldsymbol{\delta}^{(e)} = F^{(e)} \tag{24}$$

Where:

$$\boldsymbol{K}^{(e)} = \int_{V_{(e)}} \mathbf{B}^T (\square\ \boldsymbol{\Xi\Lambda}) \mathbf{B}\ dV \tag{25}$$

$$F^{(e)} = \int_{A^{(e)}} \mathbf{N}^T \Gamma dV \quad , \quad \Gamma = \begin{bmatrix} \Gamma_r \\ 0 \end{bmatrix} \tag{26}$$

Γ_r is defined as follows:

$$\Gamma_r = \rho r \omega^2 = \square\ \mathfrak{R}\, r\omega^2 \tag{27}$$

Therefore, the finite element form of the governing Equations of FG thick hollow cylinder will written as:

$$\mathbf{K}\boldsymbol{\delta} = F \tag{28}$$

5 RESULTS

5.1. Verification of Solving Method

To validate the results of this study, a comparison was made between the radial displacement findings of the current research and those obtained from ANSYS WORKBENCH ("Fig. 4"). Accordingly, in relationships, it is assumed that (n_r, n_z) are zero. Therefore, the cylinder is homogeneous and is made of m_2. The following parameters were used for validation.

a=1 (m), b=1.5 (m), L=1, E=69GPa, ρ=2715, ω =100 rad/s and ν =0.3.

A good agreement was observed for the radial displacement of the cylinder at z=$\frac{L}{2}$.

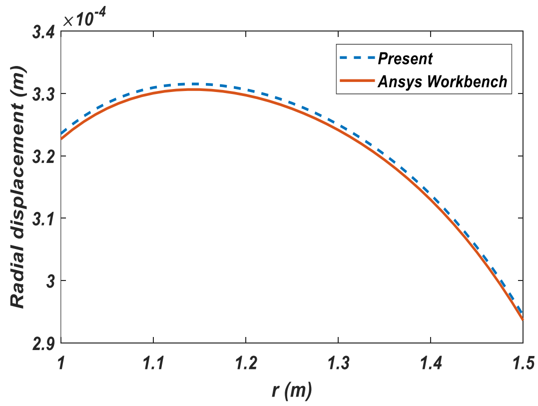

Fig. 4 Comparison between the radial displacement of the present study and Ansys Workbench.

5.2. Numerical Results

Numerical results have been studied for 2D-FGM rotating thick hollow cylinders. The effects of angular velocity and various power law exponents on the displacements and stress distributions have been investigated. The values of the parameters are:

a=1 (m), b=1.5 (m), L=1 (m),
ω =100 rad/s and ν =1/3.

The effect of the different power law exponents on the radial displacement at z=$\frac{L}{2}$ of the simply supported 2D-FGM thick hollow cylinder is depicted in "Fig. 5".

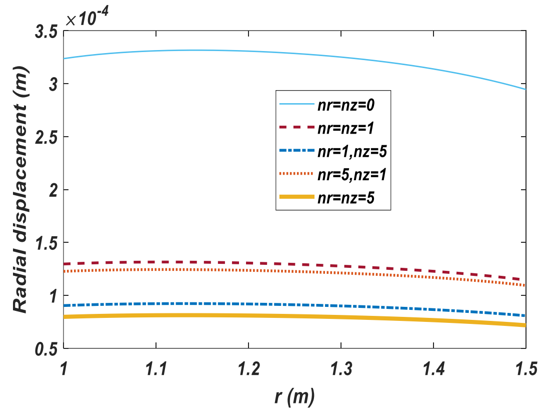

Fig. 5 Radial displacement at z=L/2 for different power law exponents.

It can be seen that the maximum radial displacement belongs to $n_r = n_z$=0. In this case, the cylinder is made of m_2, and it has minimum stiffness. Also, the minimum displacement occurs for $n_r = n_z$=5 with maximum stiffness. Figures 6-8 explain the effect of power law exponents on the radial, tangential, and axial stresses at z=$\frac{L}{2}$, respectively. Results show that the axial stresses are less affected by power law exponents, but tangential and radial stresses are mainly affected. Also, results show that maximum and minimum stresses belong to n_r=5, n_z=1, and n_r=n_z=0, respectively.

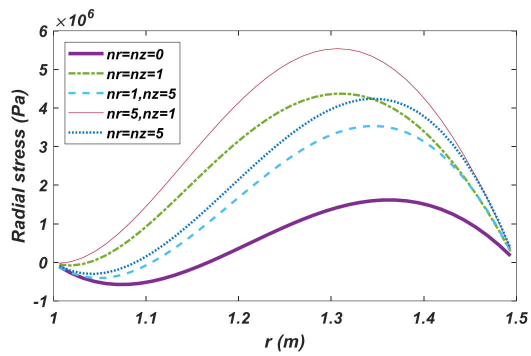

Fig. 6 Radial stress at z=L/2 for different power law exponents.

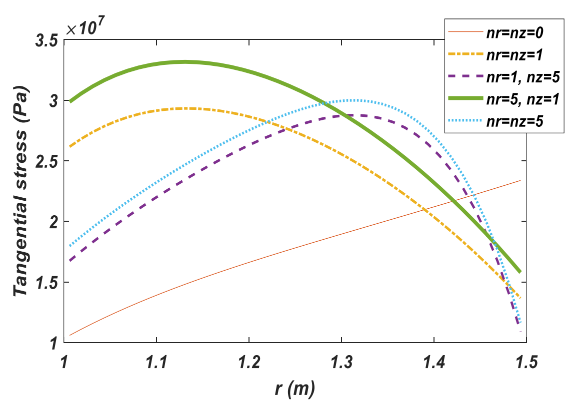

Fig. 7 Tangential stress at z=L/2 for different power law exponents.

Fig. 8 Distribution of the axial stress at z=L/2 for different power law exponents.

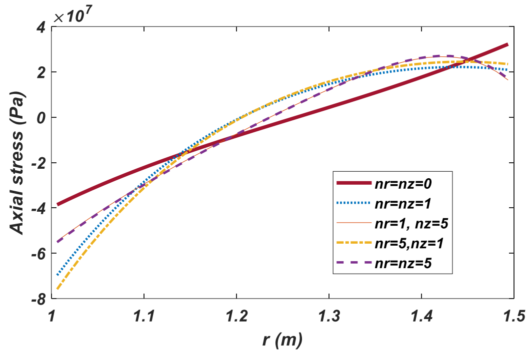

Distribution of radial displacement, radial, tangential, and axial stresses for power law exponents n_r=1, n_z=5 are shown in "Fig. 9". The effect of the circular velocity on the radial stress at z=$\frac{L}{2}$ for the simply supported 2D-FGM thick hollow cylinder is shown in "Fig. 10". Radial stress is increased as angular velocity increases.

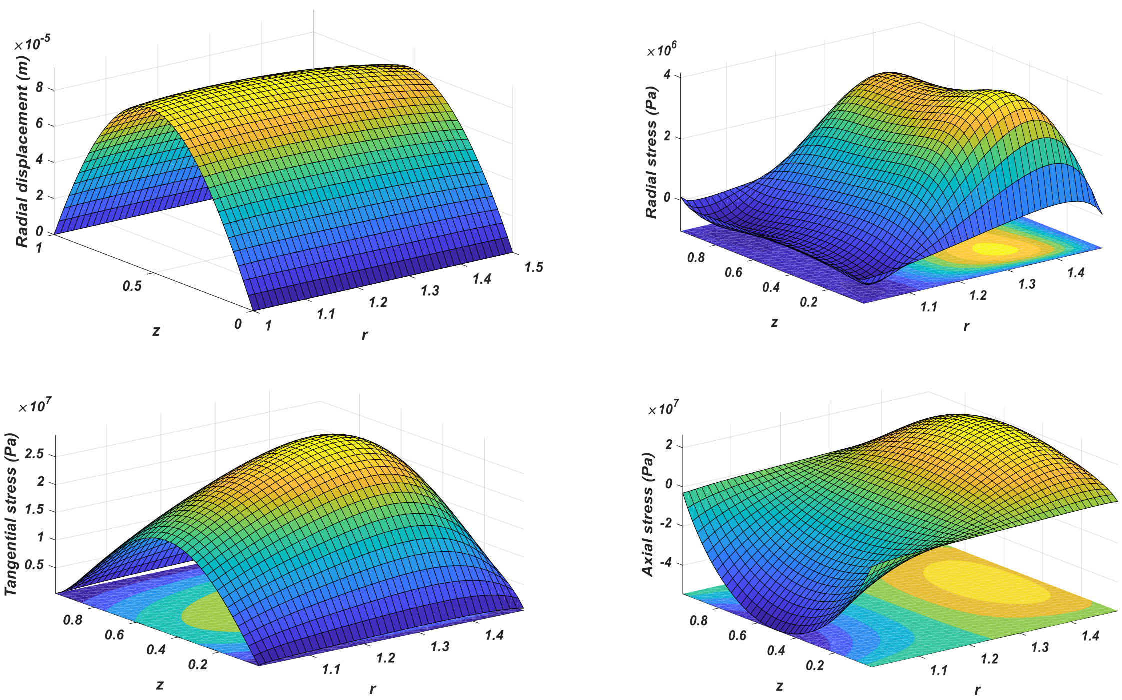

Fig. 9 Radial displacement, radial, tangential, and axial stresses for n_r=1, n_z=5.

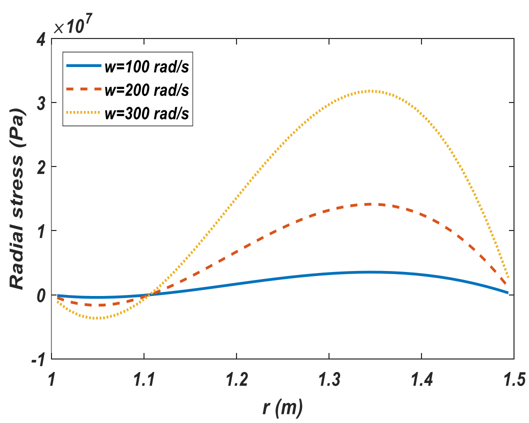

Fig. 10 Radial stress at z=L/2 for different rotational velocities.

6 CONCLUSIONS

This pioneering analysis introduces 2D axisymmetric elasticity modeling to evaluate stress distributions in rotating two-dimensional functionally graded thick hollow cylinders for the first time. The graded finite element method and Rayleigh-Ritz energy formulation were strategically employed to solve governing Equations.

The effects of power law exponents and angular velocity on displacement and stress distributions were examined.

Based on the results, 2D-FGM utilization leads to a better design to control both the maximum stresses and stress distribution by changing the material distribution. The main results of the present study are:

- Maximum radial displacement belongs to $n_r=n_z=0$. Also, the minimum displacement belongs to $n_r=n_z=5$ with maximum stiffness.
- The axial stresses are less affected by power law exponents, but tangential and radial stresses are mainly affected. Also, maximum and minimum stresses belong to $n_r=5$, $n_z=1$, and $n_r=n_z=0$, respectively.
- Radial stress increased by increasing the angular velocity.

APPENDIX A

$$\frac{\partial N_1}{\partial r}=\frac{-z_{23}[r_{46}(z-z_6)-z_{46}(r-r_6)]-z_{46}[r_{23}(z-z_3)-z_{23}(r-r_3)]}{(r_{23}z_{13}-z_{23}r_{13})(r_{46}z_{16}-z_{46}r_{16})}$$

$$\frac{\partial N_1}{\partial z}=\frac{r_{23}[r_{36}(z-z_6)-z_{36}(r-r_6)]+r_{46}[r_{13}(z-z_3)-z_{13}(r-r_3)]}{(r_{23}z_{13}-z_{23}r_{13})(r_{46}z_{16}-z_{46}r_{16})}$$

$$\frac{\partial N_2}{\partial r}=\frac{-z_{31}[r_{54}(z-z_4)-z_{54}(r-r_4)]-z_{54}[r_{31}(z-z_1)-z_{31}(r-r_1)]}{(r_{21}z_{51}-z_{21}r_{51})(r_{21}z_{51}-z_{21}r_{43})}$$

$$\frac{\partial N_2}{\partial z}=\frac{r_{31}[r_{54}(z-z_4)-z_{54}(r-r_4)]+r_{54}[r_{21}(z-z_1)-z_{31}(r-r_1)]}{(r_{21}z_{21}-z_{31}r_{21})(r_{54}z_{24}-z_{54}r_{24})}$$

$$\frac{\partial N_3}{\partial r}=\frac{-z_{21}[r_{56}(z-z_6)-z_{56}(r-r_6)]-z_{56}[r_{21}(z-z_1)-z_{21}(r-r_1)]}{(r_{21}z_{31}-z_{21}r_{31})(r_{56}z_{36}-z_{56}r_{36})}$$

$$\frac{\partial N_3}{\partial z}=\frac{r_{21}[r_{56}(z-z_6)-z_{56}(r-r_6)]+r_{56}[r_{21}(z-z_1)-z_{21}(r-r_1)]}{(r_{21}z_{31}-z_{21}r_{31})(r_{56}z_{36}-z_{56}r_{36})}$$

$$\frac{\partial N_4}{\partial r}=\frac{-z_{21}[r_{23}(z-z_3)-z_{22}(r-r_2)]-z_{23}\left(r_{31}(z-z_1)-z_{31}(r-r_4)\right)}{(r_{31}z_{41}-z_{31}r_{41})(r_{23}z_{43}-z_{23}r_{43})}$$

$$\frac{\partial N_4}{\partial z}=\frac{r_{21}[r_{23}(z-z_2)-z_{23}(r-r_2)]+r_{23}[r_{21}(z-z_1)-z_{31}(r-r_1)]}{(r_{21}z_{41}-z_{21}r_{41})(r_{23}z_{43}-z_{23}r_{43})}$$

$$\frac{\partial N_5}{\partial r}=\frac{-z_{31}[r_{21}(z-z_1)-z_{21}(r-r_1)]-z_{21}[r_{31}(z-z_1)-z_{31}(r-r_1)]}{(r_{21}z_{51}-z_{21}r_{51})(r_{21}z_{51}-z_{21}r_{43})}$$

$$\frac{\partial N_5}{\partial z}=\frac{r_{31}[r_{21}(z-z_1)-z_{21}(r-r_1)]+\mathrm{r}_{21}[\mathrm{r}_{21}(\mathrm{z}-\mathrm{z}_1)-\mathrm{z}_{31}(\mathrm{r}-\mathrm{r}_1)]}{(\mathrm{r}_{31}\mathrm{z}_{51}-\mathrm{z}_{31}\mathrm{r}_{51})(\mathrm{r}_{21}\mathrm{z}_{51}-\mathrm{z}_{21}\mathrm{r}_{51})}$$

$$\frac{\partial \mathrm{N}_6}{\partial \mathrm{r}}=\frac{-\mathrm{z}_{21}[\mathrm{r}_{23}(\mathrm{z}-\mathrm{z}_3)-\mathrm{z}_{23}(\mathrm{r}-\mathrm{r}_3)]-\mathrm{z}_{21}[\mathrm{r}_{21}(\mathrm{z}-\mathrm{z}_1)-\mathrm{z}_{31}(\mathrm{r}-\mathrm{r}_1)]}{(\mathrm{r}_{21}\mathrm{z}_{61}-\mathrm{z}_{21}\mathrm{r}_{61})(\mathrm{r}_{23}\mathrm{z}_{63}-\mathrm{z}_{23}\mathrm{r}_{63})}$$

$$\frac{\partial \mathrm{N}_6}{\partial \mathrm{z}}=\frac{\mathrm{r}_{21}[\mathrm{r}_{23}(\mathrm{z}-\mathrm{z}_3)-\mathrm{z}_{23}(\mathrm{r}-\mathrm{r}_3)]+\mathrm{r}_{23}[\mathrm{r}_{31}(\mathrm{z}-\mathrm{z}_1)-\mathrm{z}_{31}(\mathrm{r}-\mathrm{r}_1)]}{(\mathrm{r}_{21}\mathrm{z}_{61}-\mathrm{z}_{21}\mathrm{r}_{61})(\mathrm{r}_{23}\mathrm{z}_{63}-\mathrm{z}_{23}\mathrm{r}_{63})}$$

Parameters

a	inner radius of cylinder
b	outer radius of cylinder
L	cylinder length
$\mathrm{n_r}$	nonnegative radial volume fraction exponents
$\mathrm{n_z}$	nonnegative axial volume fraction exponents
Vc_1	volume fraction of first ceramic
Vc_2	volume fraction of second ceramic
Vm_1	volume fraction of first metal
Vm_2	volume fraction of second metal
E_i	modulus of elasticity of i^{th} node
ρ_i	mass density of i^{th} node
□	vectors of shape functions
$\boldsymbol{\Xi}$	modulus of elasticity of each element
$\mathfrak{R}$	mass densities of each element
$V^{(e)}$	volume of the element
Γ	body force vector due to rotational velocity
Γ_r	components of body force in the r-direction

REFERENCES

[1] Shi, P., Xie, J., Exact Solution of Magneto-Elastoplastic Problem of Functionally Graded Cylinder Subjected to Internal Pressure, Applied Mathematical Modelling, Vol. 123, 2023, pp. 835-855,

[2] Li, X., Xie, J., and Shi, P., Magneto-Thermal–Mechanical Analysis of Functionally Graded Rotating Cylinder and Circular Disk, Archive of Applied Mechanics, Vol. 93, 2023, pp. 1449-1457.

[3] Yarımpabuç, D., Çalıskan, A. J. C. M., Computations, Applications: An International Journal, "Elastic Analysis of Functionally Graded Rotating Pressurized Cylinders, Vol. 15, 2023.

[4] Daghigh, V., Edalati, H., Daghigh, H., Belk, D. M., and Nikbin, K., Time-Dependent Creep Analysis of Ultra-High-Temperature Functionally Graded Rotating Disks of Variable Thickness, Forces in Mechanics, Vol. 13, 2023, pp. 100235.

[5] Seddighi, H., Ghannad, M., and Loghman, A.,Creep Behavior of Cylinders Subjected to an Internal Pressure and a Two Dimensional Temperature Field Using First Order Shear Deformation Theory, Journal of Solid Mechanics, Vol. 15, 2023, pp. 327-342.

[6] Omidi Bidgoli, M., Loghman, A., Arefi, M., and Faegh, R. K., Transient Stress and Deformation Analysis of A Shear Deformable FG Rotating Cylindrical Shell Made of AL-SIC Subjected to Thermo-Mechanical Loading, Australian Journal of Mechanical Engineering, Vol. 21, 2023, pp. 279-294.

[7] Maitra, K., Singh Parihar, R., Finite Element Analysis of Rotating Truncated Functionally Graded Conical Shell, Current Materials Science: Formerly: Recent Patents on Materials Science, Vol. 16, 2023, pp. 62-71.

[8] Saadatfar, M., Babazadeh, M. A., and Babaelahi, M., Creep Analysis in A Rotating Variable Thickness Functionally Graded Disc with Convection Heat

Transfer and Heat Source, Mechanics of Time-Dependent Materials, 2023.

[9] Babaei, M., Asemi, K., and Kiarasi, F., Dynamic Analysis of Functionally Graded Rotating Thick Truncated Cone Made of Saturated Porous Materials, Thin-Walled Structures, Vol. 164, 2021, pp. 107852.

[10] Xu, C., Yu, Z. X., and Du, F., Dynamic Analysis of A Thick Hollow Cylinder Made of Two-Dimensional Functionally Graded Material Using Time-Domain Spectral Element Method, Mechanics of Advanced Materials and Structures, Vol. 26, 2019, pp. 1518-1535.

[11] Yarımpabuç, D., Transient-Thermoelastic Analysis of Periodically Rotated Functionally Graded Hollow Cylinder, Journal of Engineering Mathematics, Vol. 128, 2021, pp. 18.

[12] Jabbari and M., Nejad, M. Z., Mechanical and Thermal Stresses in Radially Functionally Graded Hollow Cylinders with Variable Thickness Due to Symmetric Loads, Australian Journal of Mechanical Engineering, Vol. 18, 2020, pp. S108-S121.

[13] Mehditabar, A., Rahimi, G. H., and Tarahhomi, M. H., Thermo-Elastic Analysis of A Functionally Graded Piezoelectric Rotating Hollow Cylindrical Shell Subjected to Dynamic Loads, Mechanics of Advanced Materials and Structures, Vol. 25, 2018, pp. 1068-1079.

[14] Gharibi, M., Zamani Nejad, M., and Hadi, A., Elastic Analysis of Functionally Graded Rotating Thick Cylindrical Pressure Vessels with Exponentially-Varying Properties Using Power Series Method of Frobenius, Journal of Computational Applied Mechanics, Vol. 48, 2017, pp. 89-98.

[15] Jabbari, M., Nejad, M. Z., and Ghannad, M., Thermo-Elastic Analysis of Axially Functionally Graded Rotating Thick Cylindrical Pressure Vessels With Variable Thickness Under Mechanical Loading, International Journal of Engineering Science, Vol. 96, 2015, pp. 1-18.

[16] Jafari Fesharaki, J., Jafari Fesharaki, V., Yazdipoor, M., and Razavian, B., Two-Dimensional Solution for Electro-Mechanical Behavior of Functionally Graded Piezoelectric Hollow Cylinder, Applied Mathematical Modelling, Vol. 36, 2012, pp. 5521-5533.

[17] Zafarmand, H., Hassani, B., Analysis of Two-Dimensional Functionally Graded Rotating Thick Disks with Variable Thickness, Acta Mechanica, Vol. 225, 2014, pp. 453-464.

[18] Dai, H. L., Dai, T., and Zheng, H. Y., Stresses Distributions in A Rotating Functionally Graded Piezoelectric Hollow Cylinder, Meccanica, Vol. 47, 2012, pp. 423-436.

[19] Shishesaz, M., Hosseini, M., Naderan Tahan, K., and Hadi, A., Analysis of Functionally Graded Nanodisks Under Thermoelastic Loading Based on The Strain Gradient Theory, Acta Mechanica, Vol. 228, 2017, pp. 4141-4168.

[20] Koohi Faegh Dehkourdi, R., Omidi Bidgoli, M., and Hosseini, M., A Case Study on the Influence of Friction Coefficient and Rotational Speed on Transient Thermoelastic Response of FGM Rotating Cylinder %J Mechanics Of Advanced Composite Structures, Mechanics Of Advanced Composite Structures, Vol. 9, 2022, pp. 399-408.

[21] Babaei, M., Kiarasi, F., Asemi, K., and Hosseini, M., Functionally Graded Saturated Porous Structures: A Review, Journal of Computational Applied Mechanics, Vol. 53, 2022, pp. 297-308.

[22] Shishesaz, M., Hosseini, M., Mechanical Behavior of Functionally Graded Nano-Cylinders Under Radial Pressure Based on Strain Gradient Theory, Journal of Mechanics, Vol. 35, 2018, pp. 441-454.

[23] Nejad, M. Z., Hadi, A., Non-Local Analysis of Free Vibration of Bi-Directional Functionally Graded Euler–Bernoulli Nano-Beams, International Journal of Engineering Science, Vol. 105, 2016, pp. 1-11.

[24] Shariati, M., Shishesaz, M., Mosalmani, R., Seyed Roknizadeh, S. A., and Hosseini, M., Nonlocal Effect on The Axisymmetric Nonlinear Vibrational Response of Nano-Disks Using Variational Iteration Method, Journal of Computational Applied Mechanics, Vol. 52, 2021, pp. 507-534.

[25] Barati, A., Hadi, A., Nejad, M. Z., and Noroozi, R., On Vibration of Bi-Directional Functionally Graded Nanobeams Under Magnetic Field, Mechanics Based Design of Structures and Machines, Vol. 50, 2022, pp. 468-485.

[26] Mohammadi, M., Hosseini, M., Shishesaz, M., Hadi, A., and Rastgoo, A., Primary and Secondary Resonance Analysis of Porous Functionally Graded Nanobeam Resting on A Nonlinear Foundation Subjected to Mechanical and Electrical Loads, European Journal of Mechanics - A/Solids, Vol. 77, 2019, pp. 103793.

[27] Haghshenas Gorgani, H., Mahdavi Adeli, M., and Hosseini, M., Pull-in Behavior of Functionally Graded Micro/Nano-Beams for MEMS and NEMS switches, Microsystem Technologies, Vol. 25, 2019, pp. 3165-3173.

[28] Hosseini, M., Hadi, A., Malekshahi, A., and Shishesaz, M., A Review of Size-Dependent Elasticity for Nanostructures, Journal of Computational Applied Mechanics, Vol. 49, 2018, pp. 197-211.

[29] kiarasi, F., babaei, M., Sarvi, P., asemi, K., hosseini, M., and Omidi Bidgoli, M., A Review on Functionally Graded Porous Structures Reinforced by Graphene Platelets, Journal of Computational Applied Mechanics, Vol. 52, 2021, pp. 731-750.

[30] Shariati, M., Shishesaz, M., Sahbafar, H., Pourabdy, M., and Hosseini, M., A Review on Stress-Driven Nonlocal Elasticity Theory, Journal of Computational Applied Mechanics, Vol. 52, 2021, pp. 535-552.

[31] M. Khatoonabadi, M. Jafari, F. Kiarasi, M. Hosseini, M. Babaei, and K. Asemi, "Shear buckling response of FG porous annular sector plate reinforced by graphene platelet subjected to different shear loads %J Journal of Computational Applied Mechanics," vol. 54, pp. 68-86, 2023.

[32] Daneshmehr, A., Rajabpoor, A., and Hadi, A., Size Dependent Free Vibration Analysis of Nanoplates Made of Functionally Graded Materials Based on Nonlocal Elasticity Theory with High Order Theories, International Journal of Engineering Science, Vol. 95, 2015, pp. 23-35.

[33] Barati, A., Mousavi Khoram, M., Shishesaz, M., and Hosseini, M., Size-Dependent Thermoelastic Analysis of Rotating Nanodisks of Variable Thickness, Journal of Computational Applied Mechanics, Vol. 51, 2020, pp. 340-360.

[34] Shishesaz, M.,, Shariati, M., and Hosseini, M., Size-Effect Analysis on Vibrational Response of Functionally Graded Annular Nano-Plate Based on Nonlocal Stress-Driven Method, International Journal of Structural Stability and Dynamics, pp. 2250098.

[35] Barati, A., Adeli, and M. M., Hadi, A., Static Torsion of Bi-Directional Functionally Graded Microtube Based on the Couple Stress Theory Under Magnetic Field, International Journal of Applied Mechanics, Vol. 12, 2020, pp. 2050021.

[36] Hosseini, M., Shishesaz, M., Tahan, K. N., and Hadi, A., Stress Analysis of Rotating Nano-Disks of Variable Thickness Made of Functionally Graded Materials, International Journal of Engineering Science, Vol. 109, 2016, pp. 29-53.

[37] Hosseini, M., Shishesaz, M., and Hadi, A., Thermoelastic Analysis of Rotating Functionally Graded Micro/Nanodisks of Variable Thickness, Thin-Walled Structures, Vol. 134, 2019, pp. 508-523.

[38] Noroozi, R., Barati, A., Kazemi, A., Norouzi, S., and Hadi, A., Torsional Vibration Analysis of Bi-Directional FG Nano-Cone with Arbitrary Cross-Section Based on Nonlocal Strain Gradient Elasticity, Advances in Nano Research, Vol. 8, 2020, pp. 13-24.

[39] Zarezadeh, E., Hosseini, V., and Hadi, A., Torsional Vibration of Functionally Graded Nano-Rod Under Magnetic Field Supported by A Generalized Torsional Foundation Based on Nonlocal Elasticity Theory, Mechanics Based Design of Structures and Machines, 2019, pp. 1-16.

[40] Mahmoudi, R., Barati, A., Hosseini, M., and Hadi, A., Torsional Vibration of Functionally Porous Nanotube Based on Nonlocal Couple Stress Theory, International Journal of Applied Mechanics, pp. 2150122.

[41] Adeli, M. M., Hadi, A., Hosseini, M., and Gorgani, H. H., Torsional Vibration of Nano-Cone Based on Nonlocal Strain Gradient Elasticity Theory, The European Physical Journal Plus, Vol. 132, 2017, pp. 393.

[42] Mohammadi, M., Farajpour, A., Moradi, A., and Hosseini, M., Vibration Analysis of The Rotating Multilayer Piezoelectric Timoshenko Nanobeam, Engineering Analysis with Boundary Elements, Vol. 145, 2022, pp. 117-131.

[43] Shariati, M., Hosseini, M., and Nakhli sahraei, M., Vibration of Nano-Disks Using Adomian Decomposition Method Based on Nonlocal Mindlin Plate Theory, presented at the The 30th Annual International Conference of Iranian Society of Mechanical Engineers Iran, Tehran, 2022.

[44] Hadi, A., Nejad, M. Z., and Hosseini, M., Vibrations of Three-Dimensionally Graded Nanobeams, International Journal of Engineering Science, Vol. 128, 2018, pp. 12-23.